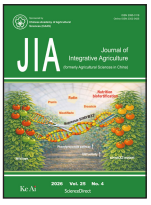
Journal of Integrative Agriculture 2026, 25(4): 1402–1417

Available online at ScienceDirect

Journal of Integrative Agriculture



RESEARCH ARTICLE

Proteomic investigation reveals the molecular mechanisms of plant height regulation in foxtail millet

Zhiying Zhao[2*], Wanting Li[1*], Yifei Wang[1], Meng Jin[2, 3], Wenqiang Tang[1], Jiayi Li[1], Renliang Zhang[2], Yaxian Zhang[1], Peiyong Xin[4, 5], Jinfang Chu[4, 5], Yingjie Gao[1], Sha Tang[2#], Xianmin Diao[2#], Baowen Zhang[1#]

[1] *Key Laboratory of Molecular and Cellular Biology, Ministry of Education/Hebei Research Center of the Basic Discipline of Cell Biology/Hebei Collaboration Innovation Center for Cell Signaling and Environmental Adaptation/Hebei Key Laboratory of Molecular and Cellular Biology/College of Life Sciences, Hebei Normal University, Shijiazhuang 050024, China*

[2] *Institute of Crop Sciences, Chinese Academy of Agricultural Sciences, Beijing 100081, China*

[3] *National Key Laboratory of Wheat Improvement/College of Life Sciences, Shandong Agricultural University, Tai'an 271018, China*

[4] *National Centre for Plant Gene Research (Beijing)/Institute of Genetics and Developmental Biology, Chinese Academy of Sciences, Beijing 100101, China*

[5] *University of Chinese Academy of Sciences, Beijing 100049, China*

Highlights

- Proteomics of internode, node and leaf at jointing stage explains plant height.
- Auxin signaling activates the auxin response factor (ARF)–small auxin up RNA (SAUR) module to promote internode elongation.
- Two SiSAUR-like haplotypes are linked to plant height and separated by a marker.

Abstract

Plant height is an essential characteristic of agronomic traits, and an ideal plant height is essential for achieving high crop yields. Foxtail millet (*Setaria italica*) has become a novel diploid C_4 model crop. The proteomic profiles of the internode, node, and leaf in two foxtail millet varieties with different heights, Ci846 and Yugu 18, were investigated at the jointing stage in this study. There were different degrees of enrichment in various processes, such as plant hormone signal transduction, the MAPK signaling pathway, and others. In particular, the proper content of auxin could activate downstream SiARFs-SiSAURs expression, which enhances the length of internodes. Haplotype analysis of SiSAUR-like revealed two differential haplotypes of associated plant height, Hap1 and Hap2. The molecular marker SiSAUR-like-FCM1-2 can effectively separate materials into Hap1 and Hap2. Two additional genes, designated *SiGH3* and *SiTCH4*, were found to be associated with plant height regulation. In conclusion, this study not only uncovers the crucial role of auxin regulators in modulating plant height during the jointing stage but also provides molecular markers that will be invaluable for molecular breeding efforts. The findings of this research help to elucidate the molecular mechanisms of plant height determination that can be used for crop variety innovation and breeding.

Keywords: plant height, proteomics, foxtail millet, auxin, molecular marker

1. Introduction

Plant height is an essential factor affecting crop architecture, lodging resistance, high-density stress, and yield. The genes and pathways controlling plant height can be roughly classified into two known types: (1) genes related to the biosynthesis or signal transduction of gibberellins (GAs), brassinosteroids (BRs), strigolactones (SLs), auxin, cytokinin (CTK), abscisic acid (ABA) and ethylene (ETH); and (2) genes related to non-hormonal pathways, including cell wall development, cell division, RNA editing, the cytosolic

Received 13 March 2024; Received in revised form 26 April 2024; Accepted 9 May 2024; Available online 27 June 2024
Zhiying Zhao, E-mail: zhiyingzh@126.com; Wanting Li, E-mail: lwting0215@163.com; #Correspondence Baowen Zhang, Tel: +86-311-80787594, E-mail: zhangbw@hebtu.edu.cn; Xianmin Diao, E-mail: diaoxianmin@caas.cn; Sha Tang, E-mail: tangsha@caas.cn
* These authors contributed equally to this study.

© 2026 CAAS. Publishing services by Elsevier B.V. on behalf of KeAi Communications Co. Ltd. This is an open access article under the CC BY-NC-ND license (http://creativecommons.org/licenses/by-nc-nd/4.0/). Peer review under responsibility of Editorial Board of *Journal of Integrative Agriculture*.
doi: 10.1016/j.jia.2024.06.014

glutamine synthetic pathway, fatty acid metabolism, and ubiquitin-proteasome pathway; in addition to some uncharacterized pathways (Liu *et al.* 2018; Miao *et al.* 2024).

Studies have shown that many genes that regulate plant height are active in the most widely cultivated cereal crops, such as rice, wheat, and maize. The most famous of these are the 'green revolution' genes *Semidwarf1* (*SD1*) and *Reduced height* (*RHT*), which are found in rice and wheat and are involved in the biosynthesis and signaling of GA, respectively (Peng *et al*. 1999; Sasaki *et al.* 2002; Spielmeyer *et al.* 2002; Wu *et al.* 2011; Van De Velde *et al.* 2021). Mutants defective in or overexpressing the genes of GA biosynthesis and signaling, including *dwarf1* (*d1*), *d3*, *ZmGA3ox2*, *ZmGA20ox1*, *TaGA2oxA9*, and *OsGID2*, show various degrees of change in plant height (Winkler and Helentjaris 1995; Sasaki *et al.* 2003; Teng *et al.* 2013; Voorend *et al.* 2016; Würschum *et al.* 2017; Ford *et al.* 2018; Tian *et al.* 2022). GAs are recognized as the most significant plant hormones influencing plant height, although other hormones are also involved in regulating plant height. Components of BR synthesis or signaling, such as *OsDWARF11*, *ZmDET2*, *ZmDWARF1, ZmBRI1*, *OsBRI1*, *OsBSK3*, and *OsBSK1-1*, have been knocked out or downregulated, resulting in severe dwarf phenotypes (Tanabe *et al.* 2005; Hartwig *et al.* 2011; Kir *et al.* 2015; Best *et al.* 2016; Zhang *et al.* 2016; Tian *et al.* 2023). In addition, auxin receptor OsTIR1/AFB, auxin transporter ZmPIN1a, auxin response factor TaARF12, and others have also been implicated in the genetic control of plant height (Ashikari *et al.* 2005; Yang *et al.* 2012; Li *et al.* 2018, 2020; Shi *et al.* 2020; Guo *et al.* 2021). Nevertheless, the role of related components of the plant hormone signal transduction pathway in plant height regulation still needs to be further explored, especially regarding BR and auxin, which regulate plant elongation and development.

Foxtail millet (*Setaria italica*) is one of the most broadly cultivated cereal crops in China and is known for resistance to drought, salt, and other abiotic stresses, and survival in nutrient-poor soil (Diao and Jia 2017). With the publication of the reference genome sequence in 2012 and the realization of stable genetic transformation, foxtail millet has become a C_4 model crop that can be used to study the evolution, stress physiology, and biomass production of cereal crops (Zhang *et al.* 2012; Lata *et al.* 2013; Diao *et al.* 2014; Yang *et al.* 2020; Panchal *et al.* 2023). However, its relatively tall plant height makes foxtail millet prone to lodging. Several foxtail millet dwarf-related genes have been reported. For example, *SiDWARF1*, *SiDWARF2*, and *SiAGO1b* were shown to regulate plant height by interrupting either the interaction with SiGID1, the synthesis of GA, or the function of small RNA recruitment (Liu *et al.* 2016; Xue *et al.* 2016; Zhao *et al.* 2019). Furthermore, a RIL population was generated by crossing the breeding line Ai88 with the elite cultivar Liaogu 1, leading to the discovery of multiple QTLs and candidate genes through population analysis, and a significant association with GA synthesis was demonstrated (He *et al.* 2021).

Thus far, most research on plant height has focused on genome-level and genetic population analyses. However, there has been a notable lack of research on proteome levels, and only some studies on salt stress and drought stress have involved proteomics in foxtail millet (Pan *et al.* 2018, 2021). Proteomics is a clustering of protein (peptide) profiling techniques that studies protein expression, interaction, and posttranslational modification, and it has been widely used in various plant species (Huo *et al.* 2016; Zhou *et al.* 2019; Liu *et al.* 2025; Zhang *et al.* 2025). Therefore, proteomic studies of foxtail millet hold significant value in elucidating the biological mechanisms underlying plant height regulation.

To investigate the regulatory mechanisms of plant height in foxtail millet, we used Ci846 and Yugu 18, two varieties with significant differences in plant height, as the materials for this study. Since the jointing stage marks the onset of plant height development, we conducted proteomic analysis on the tissues of nodes, internodes, and leaves during this period. Many regulatory proteins in the internode, node, and leaf were identified. These results showed that proteins involved in the mitogen activated protein kinase (MAPK) signaling pathway, phytohormone signal transduction, protein processing in the endoplasmic reticulum, spliceosome, ribosome, endocytosis, carbon metabolism, biosynthesis of amino acids, and plant–pathogen interactions might play vital roles in the growth and development of foxtail millet at the jointing stage. Notably, the auxin, BR, and GA signaling pathways might play central roles in controlling plant height, and the key regulatory genes in these pathways may be crucial for regulation not only at the transcriptional level but also at the protein level. In addition, protein posttranslational modification mechanisms, including ubiquitination and phosphorylation, also play pivotal roles in regulating plant height in foxtail millet.

2. Materials and methods

2.1. Plant materials and growth conditions

The foxtail millet plants used in this study included Ci846, Yugu 18, Paoziyanguzi 1, Maotigu, Longzhuanian, Qingruangu, Xiaohonggu, Chigu 7, Ai88, Mengfenggu 11, Huangtoubang, Jigu 19, Gongai 2, Dazaopi, and Longgu 31. The plants were grown at 28°C and 55% relative humidity under long-day conditions (16 h of light at 100 μmol m^{-2} s^{-1} followed by 8 h of darkness) either in a growth room or in the experimental field of the Institute of Crop Sciences, Chinese Academy of Agricultural Sciences (116°34′E, 39°97′N, Beijing, China), during the growth period (June to October).

2.2. Sample preparation and protein extraction

A urea-based protein extraction procedure that was fine-tuned by Guo and Li (2011) was performed. The leaves, along with all nodes and internodes of plants (n>30 per biological repeat) from three independent plantings were carefully collected and used for protein extraction. Leaves, nodes, and internodes were ground into a powder in liquid nitrogen, and then pre-cooled urea extraction buffer (UEB) (Guo and Li 2011) was added at a ratio of 2 mL g^{-1}. The homogenate was filtered by two layers of Miracloth (Merck, Germany) and centrifuged at 110,000×g for 2 h to remove the plant cell debris. The supernatant was further precipitated with 3 vol of pre-cooled acetone:methanol (12:1, v/v).

Residual pigment and precipitated urea were removed from the protein pellet by the addition of a pre-cooled 10–20 vol (v/w) acetone:methanol:H_2O mix (12:1:1.4, v/v). The pellet was air-dried and quickly redissolved in 1 mL resuspension buffer (RSB) (Guo and Li 2011). The protein pellet of foxtail millet was then precipitated with 3 vol of pre-cooled acetone:methanol (12:1, v/v) and centrifuged at 12,000×g for 20 min at 4°C. The protein pellet was washed one more time after storage at –20°C for 2 h and then stored in a –80°C freezer. The protein yield was measured by weighing with Micro Balances (Sartorius, Germany) after freeze-drying.

2.3. In solution digestion of the proteins in leaves, nodes, and internodes

Parallel enzymatic digestion was conducted on 100 μg of protein extracted from the leaves, nodes, and internodes of both Yugu 18 and Ci846. The total proteins from leaves, nodes, and internodes were reduced with 5 mmol L^{-1} dithiothreitol (Thermo Fisher, USA) for 40 min at 60°C, alkylated with 15 mmol L^{-1} iodoacetamide (Merck, Germany) for 45 min at room temperature in the dark, and then digested with trypsin (5% w/w, Promega, USA) for approximately 20 h at 37°C. Trypsin was added in two 10 h intervals. Afterward, the digested peptides were desalted using a C18 SPE column (Anpel, China).

2.4. High-pH reverse separation

The desalted peptide samples were separated using a Gemini® C18 column (110 Å pore size, 5 μm particle size, 4.6 mm×150 mm, Phenomenex, USA) through high-performance liquid chromatography (HPLC) (Waters, USA). Solvent A for the liquid-phase separation was 5 mmol L^{-1} ammonium formate (Merck, Germany) at pH 10.0 in water, and solvent B was 5 mmol L^{-1} ammonium formate (Merck, Germany) at pH 10.0 in acetonitrile (ACN). The initial concentration was 98% solvent A and 2% solvent B, and the elution gradient was set from 5% solvent B at 10 min to 45% at 30 min with a flow rate of 1 mL min^{-1}. From the 10th min, the eluate was collected every 1 min. A total of 20 eluate samples were combined into five tubes, in which the 11th, 16th, 21st, and 26th tubes were combined into one tube, and the rest could be combined in the same manner. This principle of combining ensures that the physicochemical properties of the peptides in each tube are relatively far apart, which will facilitate the better separation and identification of more proteins in the later LC-MS/MS analysis. The combined peptides were dried under vacuum and stored in a –80°C freezer for further LC-MS/MS analysis.

2.5. Shotgun analysis

The digested peptides were resuspended in 20 μL of 0.1% formic acid (FA), and the concentration was measured using a Nanodrop (Thermo Fisher, USA). The concentration of each sample was adjusted to 1 μg $μL^{-1}$ using 0.1% FA. For each sample, a 2 μL aliquot was taken and separated with a UPLC M-Class system (Waters, USA). The elution gradient was set from 2% solvent B (0.1% FA in ACN) to 45% in 60 min with a C18 analytical column (1.8 μm particle size, 100 μm ID×150 mm length, Waters, USA), and the flow rate was 350 nL min^{-1}. Then the eluted peptides were analyzed by Q-Exactive HF (Thermo Fisher, USA) with 2.0 kV electro-spray, 350–1,200 *m/z* full-scan, 60,000 precursor ion resolution, 5 ms maximum ion injection time, and 27% normalized collision energy of the HCD. Profile mode was used to record the spectra. Raw data were searched using Peaks Studio 8.5, the database for the first round was Setaria italica v2.2 (https://phytozome-next.jgi.doe.gov/info/Sitalica_v2_2), and the database for the M-round was Uniprot Taxonomy Liliopsida (https://www.uniprot.org/taxonomy/4447, 23/12/2022). To maximize the detection of proteins in plant tissues, each experimental group was independently searched and aligned using the PEAKS 8.5 software, without involving a quantitative and normalization analysis between Yugu 18 and Ci846. Both the Protein Group and Peptide Sequences FDR were filtered to 1%. The Parent Mass Error Tolerance was 10.0 ppm, and the Fragment Mass Error Tolerance was 0.02 Da. In addition, the Max Missed Cleavages was set to 2. For fixed modifications, Carboxymethyl with a mass of 58.01 was applied, while for variable modifications, Oxidation (M) with a mass of 15.99 was considered.

2.6. Bioinformatic analysis

The Venn diagrams, Gene Ontology (GO) annotation, and Kyoto Encyclopedia of Genes and Genomes (KEGG) pathway analysis were performed online using BMKCloud (https://international.biocloud.net/zh/software/tools), and Yugu 1 genomic data was downloaded from Phytozome 13 (https://phytozome-next.jgi.doe.gov/). For protein-protein interaction (PPI) networks, the data were imported into the STRING database website to obtain the interaction network between each protein pair. The node and edge information was imported into Cytoscape. Betweenness was sorted to obtain the graph of the protein-protein interaction network, and the node size was adjusted according to the betweenness. Haplotype analysis was performed online using R (https://gitee.com/zhangrenl/genehapr/wikis/Home) (Zhang *et al.* 2025).

2.7. Quantification of endogenous indole-3-acetic acid (IAA)

Samples for IAA analysis were extracted and purified as previously described (Wang *et al.* 2015; Chu *et al.* 2017), with minor modifications in the detection conditions. Approximately 200 mg of internode tissue from Yugu 18 and Ci846 was ground to powder and extracted in methanol containing deuterium-labeled indole-3-acetic acid ($^2H_2$-IAA) as an internal standard for 24 h. After centrifugation, the compound was purified using an Oasis Max solid phase extraction cylinder, and a 5500 Q-Trap System (AB SCIEX, USA) was used to perform the LC analysis with an ACQUITY UPLC BEH C18 column (1.7 μm, 100 mm×2.1 mm, Waters, USA). The mobile phase solvents were 0.05% FA in water (solvent A) and 0.05% FA in acetonitrile (solvent B) with a gradient program of 0–1 min, 1% B; 1–15 min, 1% B to 25% B; 15–16 min, 25% B to 80% B; 16–17 min, 80% B; 17–18 min, 80% B to 1% B;

and 18–20 min, 1% B. The optimized electrospray ionization (ESI) operating parameters for positive mode were: IS, 5,000 V; CUR, 35 psi; TEM, 400°C; GS1, 45 psi; and GS2, 55 psi. The multiple reaction monitoring (MRM) mode was performed for quantification, and the MRM transitions were 178.0>132.0 for $^{2}H_{2}$-IAA and 176.0>130.0 for IAA. Three biological replicates were analyzed for each sample.

2.8. RNA extraction and qRT-PCR analysis of *SiSAURs*

The internodes of 6-wk-old long-day condition (16L/8D) plants were acquired from Ci846 and Yugu 18 seedlings. TRIzol (Invitrogen, USA) was used to extract the total RNA, and M-MLV (TaKaRa, Japan) was used to reverse-transcribe the *SiSAURs* cDNA according to the manufacturer's instructions. The gene-specific primers used are listed in Appendix A. Using *SiACTIN* as the internal reference, comparative C_t was used to determine the relative abundance of each target gene.

2.9. Extraction of foxtail millet leaf DNA and marker development

The cetyltrimethylammonium bromide (CTAB, Aladdin, China) method (Liang *et al.* 2023) was used to extract total genomic DNA from foxtail millet leaves with minor modifications. The quality of the extracted gDNA was evaluated with a 1% agarose gel. The polymorphic sequence marker associated with the promoter of the *SiSAUR-like* gene was developed using dCAPS Finder 2.0 (http://helix.wustl.edu/dcaps/dcaps.html). The *Hpy*99I digested PCR products were analyzed by 15.0% polyacrylamide gel electrophoresis. The dCAPS-related primers used are listed in Appendix A.

2.10. RNA-seq analysis

Stems of Ci846 and Yugu 18 were harvested at the jointing stage, with each group consisting of three biologically independent replicates. These samples were promptly frozen in liquid nitrogen to preserve RNA integrity for subsequent total RNA isolation and cDNA library construction. RNA-seq analysis was conducted using the Illumina HiSeq.2000 platform in a 100 bp paired-end mode (Illumina Inc., USA), with three independent biological replications for each sample. Differentially expressed genes (DEGs) were identified using a significance threshold of *P*-value<0.05 and a fold change criterion of >2 or <0.5.

2.11. Statistical analysis

Student's *t*-test and one-way analysis of variance (ANOVA) with Tukey's honestly significant difference test were performed to evaluate the differences across sample groups. Statistically significant differences are indicated below by different lowercase letters (P<0.05, ANOVA test), one asterisk (P<0.05, Student's *t*-test), or two asterisks (P<0.01, Student's *t*-test), which were determined using GraphPad prism (v9.0.0).

3. Results

3.1. Phenotypes of two foxtail millets at the jointing stage

Ci846 is an easily transformed spring-sowing ecotype, and Yugu 18 is a widely grown summer-sowing variety. Our study found that these two varieties had a significant difference in plant height at the jointing stage (Fig. 1-A–C). The jointing stage, as a period of rapid internode elongation in the growth process of cereal crops, is an important period in which to study plant height. We observed that Ci846 was taller than Yugu 18 due to the greater number of internodes and the greater length of each internode (Fig. 1-D and E). In addition, the leaf length of Ci846 was greater than that of Yugu 18 (Fig. 1-F).

3.2. Shotgun analysis of Ci846 and Yugu 18 at the jointing stage

To explore the difference in plant height between Ci846 and Yugu 18, the nodes, internodes, and leaves of Ci846 and Yugu 18 at the jointing stage were subjected to proteomic analysis. To identify more proteins, we first separated these peptides by high pH–HPLC and combined the eluted samples into five fractions, and each fraction was analyzed separately by HPLC–MS/MS (Appendix B). To obtain more reliable data, we used a stringent threshold of FDR<0.01 for assessing the identified proteins (Appendices C–H).

As shown in Table 1, 15,628 peptides and 5,136 proteins were obtained from Ci846 internodes, 29,102 peptides and 7,610 proteins were obtained from Ci846 nodes, and 27,985 peptides and 6,975 proteins were obtained from Ci846 leaves. Totals of 6,895 peptides and 3,039 proteins were obtained from Yugu 18 internodes, 25,182 peptides and 6,990 proteins were obtained from Yugu 18 nodes, and 19,391 peptides and 7,315 proteins were obtained from Yugu 18 leaves. Without alternative splicing, 4,301, 6,290, 5,882, 2,650, 5,827, and 6,021 proteins were identified in these different tissues of Ci846 and Yugu 18, respectively. These protein data were used for subsequent analysis, and the results showed that 4,637, 7,252, and 7,183 proteins were identified in the internodes, nodes and leaves, respectively. The numbers of proteins identified in the internodes of Ci846, the internodes of Yugu 18, and the internodes overall were much smaller than those identified in the other tissues, which may be due to the highly specialized cells in the internodes.

Interestingly, we also found some *de novo*-only peptides that had not yet been identified in different tissues of Ci846 and Yugu 18. Considering that some proteins may not exist in the current foxtail millet transcriptome database, we conducted a second multi-round search of the *de novo*-only peptides with the monocotyledonous plant proteins database, and 629, 1,062, 565, 227, 1,210, and 839 protein groups were newly identified (Table 1; Appendices I–N). These findings further expand the database of known proteins of foxtail millet.

3.3. GO annotation and functional classification of differentially accumulated proteins between the two varieties

A comparison of the identified proteins among the internodes, nodes, and leaves showed that 3,390 proteins were coexpressed in Ci846, while 2,181 proteins were coexpressed in Yugu 18 (Appendix O-a and b). A comparison of those 3,390 and 2,181 proteins showed that 1,926 were coexpressed in both varieties, 255 were identified in Yugu 18

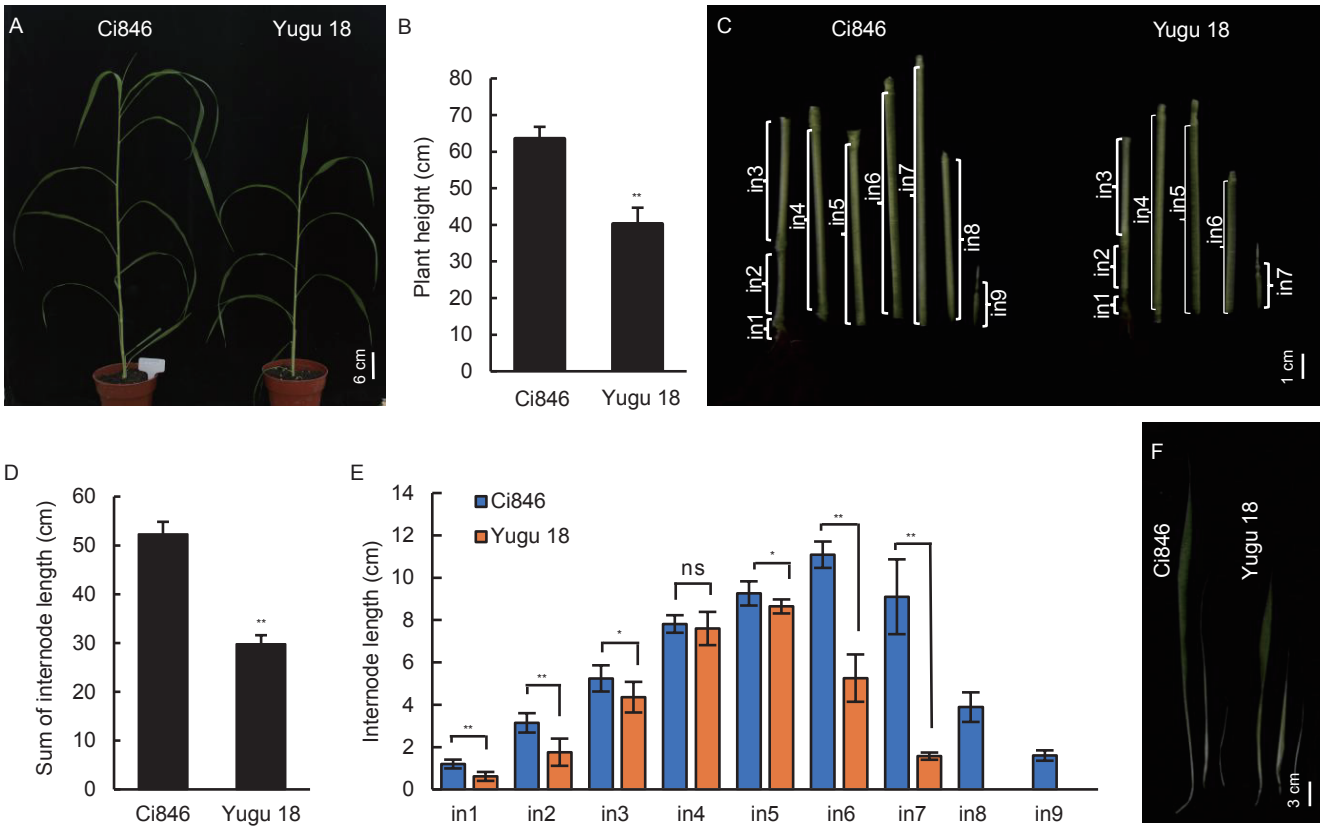


Fig. 1 Phenotype of Ci846 and Yugu 18 at the jointing stage. A, the phenotype of Ci846 and Yugu 18 seedlings at the jointing stage. B, the plant height of A. C, the node and internode (in) of A, in9 of Ci846 and in7 of Yugu 18 included apical unelongated internodes. D, the sum of internode length. E, the length of the internode. F, the youngest three leaves of A. Error bars indicate ±SD of n=7. Student's t-test were carried out to analyze significant differences between two varieties, ns indicates the P-value>0.05, * and ** indicate P-value<0.05 and <0.01, respectively.

Table 1 Overview of the identified peptide, proteins, protein groups and *de novo* only spectra of Yugu 18 and Ci846 at the jointing stage

Item[1)]	Internode		Node		Leaf	
	Ci846	Yugu 18	Ci846	Yugu 18	Ci846	Yugu 18
First round						
Peptide	15,628	6,895	29,102	25,182	27,985	19,391
Proteins	5,136	3,039	7,610	6,990	6,975	7,315
Proteins without splice variant	4,301	2,650	6,290	5,827	5,882	6,021
Protein groups	4,131	2,487	6,135	5,670	5,779	5,819
de novo only spectra	18,441	8,152	35,046	38,373	11,009	25,119
Multi-round						
Peptide	1,005	305	2,127	2,337	948	1,595
Proteins	8,477	3,038	8,211	9,579	6,274	10,089
Proteins groups	629	227	1,062	1,210	565	839

[1)] First-round indicates peptides with the foxtail millet transcriptome database; multi-round indicates *de novo* only peptides with the monocotyledonous plant proteins database.

and 1,464 were identified in Ci846 (Appendix O-c). To further characterize the functions of the identified proteins between the two varieties, we analyzed the 255 proteins identified in Yugu 18 and 1,464 proteins identified in Ci846. GO enrichment analysis indicated that the 255 identified proteins of Yugu 18 are involved principally in ubiquitin-conjugating enzyme activity, ubiquitin-like protein binding, protein polyubiquitination, protein K63-linked ubiquitination, and other processes (Appendix P-a). The 1,464 identified proteins of Ci846 are involved mainly in calcium-dependent protein serine/threonine kinase (CDPK) activity, protein phosphatase type 2A complex, phosphoprotein phosphatase activity, protein dephosphorylation, and other processes (Appendix P-b). These results suggested that the ubiquitination process is enriched in Yugu 18, while the phosphorylation and dephosphorylation processes are enriched in Ci846 during

the jointing stage.

Protein–protein interaction (PPI) network analyses revealed that two SiRUB1s (Seita.2G207500 and Seita.4G196800) were significantly enriched in Yugu 18 (Appendices P-c and Q). RUB1 (also named NEDD8) encodes a ubiquitin-like protein that is conjugated to target proteins by neddylation. Neddylation is an important posttranslational modification that covalently attaches the NEDD8 to cullins to modulate their protein activity and function (Enchev *et al.* 2015; Mergner *et al.* 2017; Schwechheimer 2018). The RUB-conjugation pathway is associated with the auxin response (Bostick *et al.* 2004). The interacting proteins of RUB1, a SiRUB1 homologous gene in *Arabidopsis*, include CUL1, CUL2, and CUL3A, which are involved in the ubiquitination and subsequent degradation of target proteins in the proteasome (Appendix P-d) (Christians *et al.* 2018). CUL1 is a component of Skp1–Cullin1–F-box protein (SCF) ubiquitin ligase complexes which take part in the molecular mechanism of the auxin response (Yu *et al.* 2015). In addition, SiPEN2 was significantly enriched in Ci846 (Appendices P-e and Q), and it is a gene that encodes a phosphatase with low *in vitro* tyrosine phosphatase activity (Gupta *et al.* 2002; Pribat *et al.* 2012). Therefore, ubiquitination and neddylation play an important role in Yugu 18, while phosphorylation and dephosphorylation are more important in Ci846. In summary, the different signaling pathways and interaction subnetworks indicated that the mechanisms regulating plant height are significantly different between Ci846 and Yugu 18 at the jointing stage.

3.4. Regulatory mechanisms of plant height in Ci846 and Yugu 18

A comparison of the identified proteins between Ci846 and Yugu 18 revealed 4,865 proteins coexpressed in the nodes of Ci846 and Yugu 18, 1,425 expressed only in the nodes of Ci846, and 962 expressed only in the nodes of Yugu 18 (Fig. 2-A). There were 4,720 proteins coexpressed in the leaves of Ci846 and Yugu 18, 1,162 expressed only in the leaves of Ci846, 1,301 expressed only in the leaves of Yugu 18 (Fig. 2-B); 2,314 coexpressed in the internodes of both Ci846 and Yugu 18, 336 expressed only in the internodes of Yugu 18, and 1,987 expressed only in the internodes of Ci846 (Fig. 2-C). A Venn diagram analysis revealed that the number of differentially expressed proteins (DEPs) in the internodes of Ci846 was significantly higher compared to Yugu 18 (1,987 *vs*. 336), in contrast to the nodes (1,425 *vs*. 962) and leaves (1,162 *vs*. 1,301). These results could be attributed to the more pronounced phenotypic differences in internodes between the two varieties, as well as the greater internode length in Ci846, which corresponds to the higher number of DEPs. This suggests that the internode tissue might be a key factor contributing to the distinct phenotypic traits observed between the two varieties.

To investigate the regulatory mechanisms of Ci846 and Yugu 18 during plant height development at the jointing stage, the KEGG pathway enrichment analysis was performed with the abovementioned proteins identified in the nodes. The results showed that the 962 and 1,425 identified proteins in Yugu 18 and Ci846 had different degrees of enrichment in processes such as plant-pathogen interaction, plant hormone signal transduction, carbon metabolism, ribosome, and others (Appendix R-a and b). Among them, 18 proteins related to hormone signal transduction were enriched in Yugu 18, and 36 such proteins were enriched in Ci846. The identified proteins in Yugu 18 covered the auxin, GA, ABA, BR, jasmonic acid (JA), and salicylic acid (SA) signaling pathways (Appendix R-c), but the identified proteins in Ci846 covered almost all hormone signaling pathways (Appendix R-d). Furthermore, several key components of the BR signaling pathway were found in Ci846, such as SiBRIs (Zhao *et al.* 2021b), SiBZR1/2 (Zhao *et al.* 2021a), and SiTCH4 (also known as SiXTH22) (Iliev *et al.* 2002).

To further investigate the molecular mechanisms that govern the plant height differences between Ci846 and Yugu 18, we conducted a GO enrichment analysis focusing on the DEPs in the nodes. The results revealed that the identified proteins in nodes of Yugu 18 participate primarily in GTP binding, GTPase activity, translation initiation factor binding, and positive regulation of translational initiation (Appendix S-a). PPI networks were constructed, which revealed the prominence of SiROP9 in Yugu 18 (Appendices Q and S-b). SiROP9 is a member of the RHO-RELATED PROTEIN GTPase gene family. Overexpressing AtRAC7/ROP9 activates ABA-induced gene expression but represses auxin-induced gene expression (Nibau *et al.* 2013). This indicates that SiROP9 may act as an important plant height regulator by integrating auxin and ABA signaling in plants. The identified proteins in nodes of Ci846 participate mainly in auxin binding, C-terminal domain (CTD) phosphatase activity, and dephosphorylation of the RNA polymerase II CT domain (Appendix S-c). Moreover, the obviously highlighted hub protein in Ci846 was SiPP2C (Appendices Q and S-d), a member of the protein phosphorylation family. This protein may take part in the negative regulation of ABA signaling pathways; for example, PP2Cs dephosphorylate SnRK2s, thereby inhibiting their activation of downstream gene expression (Brookbank *et al.* 2021). The interacting proteins of AT2G20050, a SiPP2C homologous gene in *Arabidopsis*, include BIN2, BIL1, ASK11, ASK12, ASK31, ASK41, and ASK42 (Appendix S-e), which are negative modulators of the BR signaling pathway (Yan *et al.* 2009). BIN2 also regulates plant height in wheat (Dong *et al.* 2023). Therefore, the auxin, BR, and ABA signaling pathways play crucial roles in plant height regulation.

KEGG enrichment analysis of the identified proteins in leaves revealed that the proteins of Yugu 18 are mainly associated with ABC transporters; cyanoamino acid metabolism; linoleic metabolism; nicotinate and nicotinamide metabolism; glycerophospholipid metabolism and degradation; valine, leucine and isoleucine degradation; starch and sucrose metabolism, and others (Appendix T-a). The identified proteins in the leaves of Ci846 are mainly associated with carbon metabolism, the tricarboxylic acid (TCA) cycle, oxidative phosphorylation, phosphonate and phosphinate metabolism, and others (Appendix T-b). These findings indicate that the leaf proteins of Yugu 18 are enriched in the metabolism and degradation of various amino acids

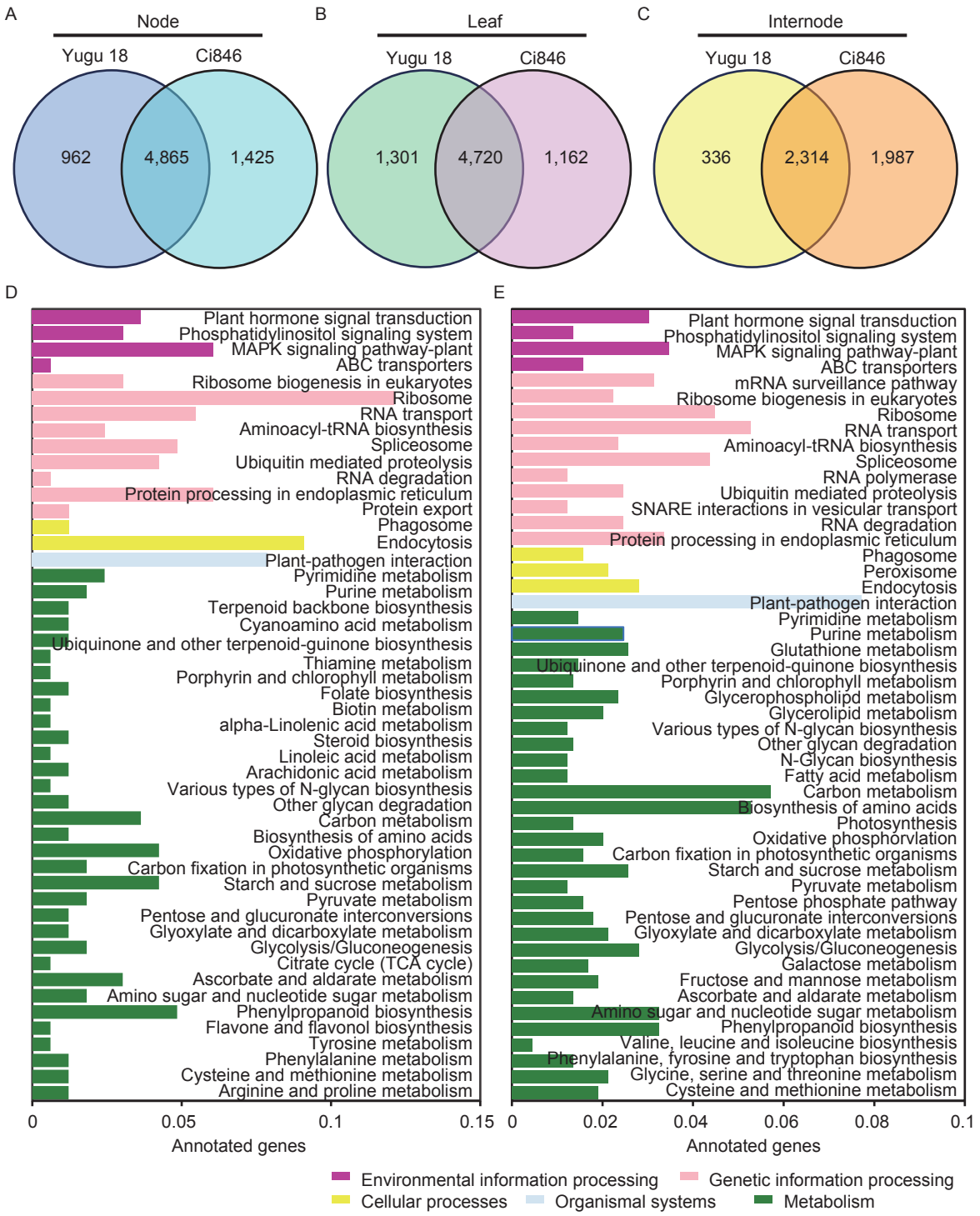


Fig. 2 Comparative analysis of identified proteins in the same tissue at the jointing stage. A–C, Venn diagrams of Ci846 and Yugu 18 regulated proteins in node (A), leaf (B), and internode (C). D and E, the Kyoto Encyclopedia of Genes and Genomes (KEGG) pathway annotation of 336 proteins in Yugu 18 internode (D) and 1,987 proteins in Ci846 internode (E).

and in the metabolism of starch and sucrose, while those in Ci846 are enriched in carbon metabolism, the TCA cycle, and phosphate and phosphate metabolism.

3.5. Auxin plays a significant role in internode-mediated plant height regulation

Since the internode number and length of Ci846 were significantly greater than those of Yugu 18 (Fig. 1), we analyzed in detail the internode proteins among the 1,987 proteins expressed only in Ci846 and 336 proteins expressed only in Yugu 18. The results revealed the significant enrichment of key proteins in multiple pathways in Ci846 compared to Yugu 18, especially in the plant hormone signal transduction pathways (Appendix U). Specifically, only six proteins

enriched in plant hormone signal transduction in Yugu 18 were involved in the ABA, BR, and SA pathways (Appendices U-a and V). In contrast, 27 proteins in Ci846 were enriched in plant hormone signal transduction, and these proteins participate in the auxin, cytokinin, ABA, ETH, BR, and SA signaling pathways (Appendices U-b and V). Among them, SiAUX1 (Seita.5G387200), SiTIR1 (Seita.9G512800) and 10 SiARFs (Seita.1G077200, Seita.1G090900, Seita.3G147000, Seita.3G179300, Seita.3G394000, Seita.4G040100, Seita.4G262300, Seita.5G321300, Seita.5G438100, and Seita.6G212000), which are components of the auxin signaling pathway, were enriched only in the internodes of Ci846 (Appendix V). Only one additional SiARF (Seita.3G020000) was enriched in Ci846 and Yugu 18, and the number of peptides in Ci846 was greater than that in Yugu 18 (Appendix V). In summary, SiAUX1, SiTIR1, and SiARFs were almost all present in the internodes of Ci846 but not in those of Yugu 18, indicating that auxin plays a very important role in regulating internode-mediated plant height. An analysis of the protein coverage of 14 SiARFs enriched in the K14486 pathway (Appendix V) revealed that almost all 11 SiARF genes in the internodes were present in Ci846 (Fig. 3-A).

To further investigate whether auxin content underlies the difference in plant height between Ci846 and Yugu 18, we conducted additional measurements of the levels of IAA, the most common and widely studied form of auxin, during the jointing stage of the two varieties. The results revealed that the IAA content in the internodes of Ci846 was significantly lower than that of Yugu 18 (Fig. 3-B). Simultaneously, we analyzed the differentially expressed genes (DEGs) in the stems of Ci846 and Yugu 18 using RNASeq. The results revealed that compared to Ci846, Yugu 18 exhibited 2,759 down-regulated DEGs and 4,971 up-regulated DEGs (Fig. 3-C; Appendix W). GO enrichment analysis showed that the 2,759 down-regulated genes are involved mainly in the response to auxin and the auxin-activated signaling pathway (Fig. 3-D; Appendix X). These auxin response genes include 11 *Small Auxin Up RNAs* (*SiSAURs*) (Appendix Y). The RNAseq data showed that the expression levels of *SiSAUR36s* (*Seita.2G295100*, *Seita.2G296700*, *Seita.2G296200*, *Seita.2G295400*, *Seita.2G296300*, *Seita.6G241400*, *Seita.2G295600*, and *Seita.6G242200*), *SiSAUR50* (*Seita.5G434800*), *SiSAUR71s* (*Seita.4G266000*, *Seita.1G075600*), and *SiSAUR72* (*Seita.6G170200*) in Yugu 18 were significantly lower than in Ci846 in stems (Fig. 4-A). In addition, qRT-PCR showed that the expression levels of *SiSAUR36s* (*Seita.6G241400*, *Seita.2G295600*, and *Seita.6G242200*), *SiSAUR71* (*Seita.4G266000)*, and *SiSAUR72* (*Seita.6G170200*) in Yugu 18 were significantly lower than in Ci846 in internodes (Fig. 4-B). These findings suggest that the proper auxin concentration can activate the downstream genes of the auxin hormone signaling pathway to regulate plant height, with SiARFs–SiSAURs playing important roles in internode-mediated plant height regulation.

3.6. Important genes contributing to genotypic variations in plant height at the jointing stage

To achieve a better understanding of the mechanism of plant height regulation at the jointing stage, we analyzed three important genes that regulate cell elongation through the auxin and BR pathways: *SiSAUR-like* (*Seita.1G161300*), *SiGH3* (*Gretchen Hagen 3*, *Seita.5G342900*), and *SiTCH4* (*Seita.4G246400*), based on proteins enriched in the plant hormone signaling pathway in our proteomic data (Appendix V).

According to the resequencing data of 1,844 foxtail millet varieties (He *et al.* 2023), all the variable loci in the promoter and CDS regions of the three genes were analyzed. Either no variation or only one amino acid variation was found in these proteins, but no variation site was associated with the plant height phenotype. However, there were abundant variation sites in the promoters of *SiSAUR-like*, *SiGH3*, and *SiTCH4*. Furthermore, 1,042 foxtail millet varieties had heterozygous or deletion sites within the 3 kb promoter of *SiSAUR-like*, and nine single-nucleotide polymorphisms (SNPs) were detected, which created nine haplotypes (Fig. 5-A). We conducted a further correlation analysis between Hap1 and Hap2, using the phenotypic data collected from multiple locations and over several years in Shanxi, Gansu, and Beijing, China. Our findings revealed that plants with the Hap1 haplotype exhibited significantly greater plant heights compared to those with the Hap2 haplotype, indicating a clear association between this haplotype and plant height (Fig. 5-B–G).

Plant height is an important agronomic trait and an important indicator in the breeding of ideal plant architecture, so it is important to develop molecular markers for plant height genes. Therefore, we developed a functional dCAPS marker (*SiSAUR-like*-FCM1-2) that permits accessions with Hap1 and Hap2 of *SiSAUR-like* using the *Hpy*99I restriction enzyme to distinguish plant height. First, we found that SNPs C/G and T/A were indeed present at position 22,811,663 of *SiSAUR-like* in Ci846 and Yugu 18 (Fig. 5-H). Following *Hpy*99I digestion, the PCR products from Ci846 accessions with greater plant height separated into 108 and 17 bp fragments, but the shorter varieties of Yugu 18 only yielded a 125 bp fragment (Fig. 5-I). Due to the relatively small size of the 17 bp band, it was not shown in the gel. We then randomly selected 13 accessions to verify the effectiveness of the *SiSAUR-like*-FCM1-2 marker (Fig. 5-I; Appendix Z). Following *Hpy*99I digestion, the PCR products of six accessions with a greater plant height of Hap1 separated into a 108 bp fragment, and the other seven accessions of Hap2 yielded a 125 bp fragment, including the known dwarf varieties Ai88 and Gongai2 (Fig. 5-I). The plant heights of each of the four varieties in Hap1 and Hap2 were randomly observed and measured, and the results indicated that the Hap1 varieties were significantly higher than those in Hap2 (Fig. 5-J and K). These banding patterns permitted the C/G of Hap1 to be distinguished from the T/A of Hap2, as well as C/G and T/A to be distinguished from other types of accessions.

Furthermore, the 1 kb promoter of *SiTCH4* had four SNPs, which created six haplotypes (Appendix AA-a). Hap1 was significantly different from Hap2 of *SiTCH4*, and the plant height of Hap2 was less than that of Hap1 in three regions of China, Hebei, Hainan, and Shanxi (Fig. 6-A–C). Hap1 and Hap2 differed by two bases, and the positions of

A

SiARFs	Internode		Node		Leaf	
	Ci846	Yugu 18	Ci846	Yugu 18	Ci846	Yugu 18
Seita.1G077200	2	0	2	3	2	3
Seita.1G090900	2	0	0	0	2	0
Seita.3G020000	10	1	25	21	15	9
Seita.3G147000	3	0	3	3	3	3
Seita.3G179300	5	0	3	3	0	3
Seita.3G394000	3	0	9	11	5	3
Seita.4G040100	2	0	4	0	2	2
Seita.4G240600	0	0	0	0	0	1
Seita.4G257800	0	0	0	0	0	2
Seita.4G262300	3	0	7	7	5	5
Seita.5G265200	0	0	2	0	2	2
Seita.5G321300	2	0	3	0	3	3
Seita.5G438100	1	0	0	0	0	0
Seita.6G212000	2	0	2	0	2	2

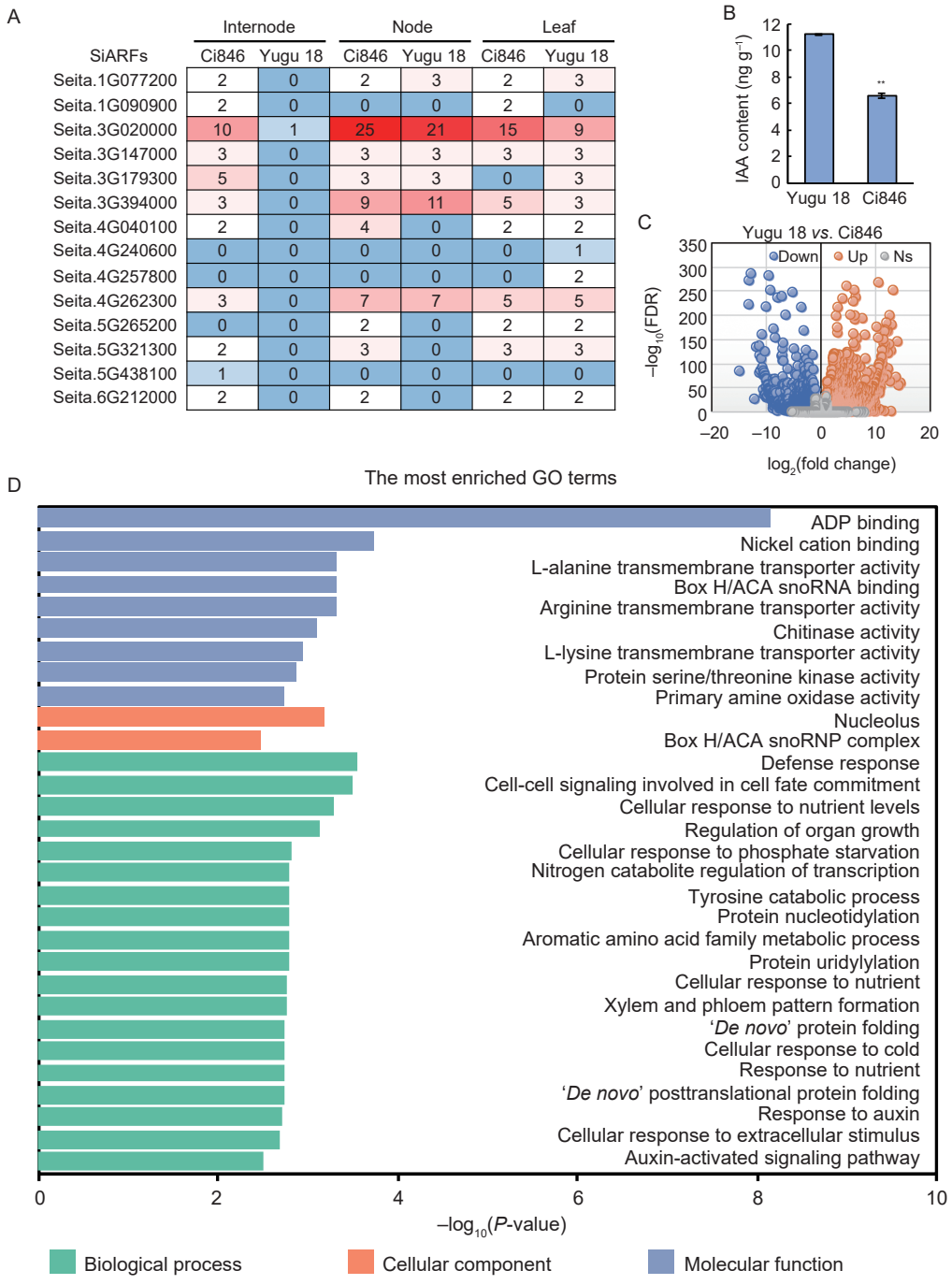


Fig. 3 Auxin content and differential genes analysis of Ci846 and Yugu 18. A, heatmap of K14486 auxin response factor's sequence coverage (%) in the internode, node, and leaf. B, indole-3-acetic acid (IAA) content in the internode of Ci846 and Yugu 18. Error bars indicate ±SD of *n*=3. Student's *t*-test were carried out to analyze significant differences between two varieties, ** indicates the *P*-value<0.01. C, differential expression genes (DEGs) number of Yugu 18 and Ci846 in the stem at the jointing stage. D, the Gene Ontology (GO) enrichment of 2,759 DEGs up-regulated by Ci846 than Yugu 18 in the stem.

these two bases were near BR response elements (BRREs), the *cis*-elements of BRs. The 3 kb promoter of *SiGH3* was also rich in variation, and 41 SNPs and two indels were found, which created 11 haplotypes (Appendix AA-b). The plant height of Hap1 was less than that of Hap2 for *SiGH3* in Hebei, Hainan, and Shanxi (Fig. 6-D–F), and that of Hap5 was less than those of Hap1 and Hap2 in Hainan (Fig. 6-E). There was only a one base difference between Hap1 and Hap2, but there was a five-base difference in Hap5. Interestingly, the Hap2 of *SiTCH4* was mainly concentrated in the northeastern part of China, but there were fewer varieties of Hap2. In contrast, Hap1 and Hap2 of *SiGH3* were distributed in the north and south of China, respectively. These results suggest that the regulatory effect on plant height of *SiTCH4* and *SiGH3* is very closely related to geographical distribution.

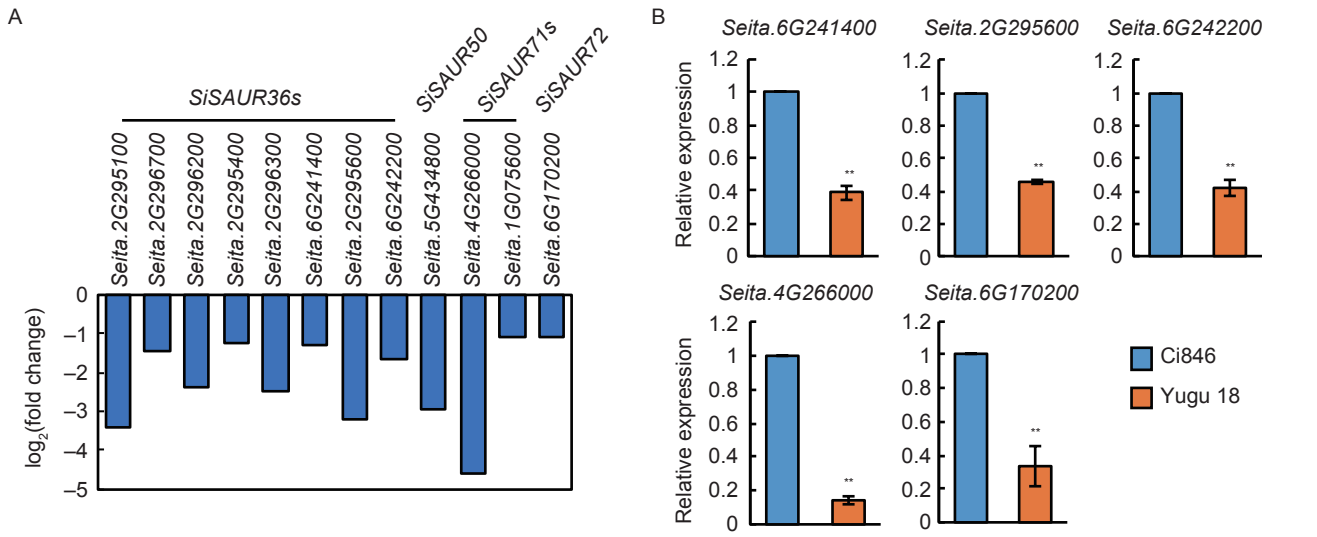


Fig. 4 Expression level of *SiSAURs* in Ci846 and Yugu 18. A, the expression level of *SiSAURs* in the stem at the jointing stage by Yugu 18 *vs.* Ci846. B, relative expression level of *SiSAURs* in internode of Ci846 and Yugu 18 at the jointing stage. Error bars indicate ±SD of n=3. Student's t-test were carried out to analyze significant differences between two varieties, ** indicates the P-value<0.01.

4. Discussion

4.1. Shotgun proteomics provides a very large number of abundant and reliable proteins

Plant height impacts lodging and is a key factor in determining crop yield. The discovery and utilization of green revolution genes in rice and wheat have led to substantial improvements in the plant architecture of these crops, resulting in significant increases in their yields (Peng *et al.* 1999; Sasaki *et al.* 2002). However, there are relatively few reports on genes related to plant height in foxtail millet, and the molecular mechanism regulating plant height remains unclear (Xue *et al.* 2016; Fan *et al.* 2017; Panchal *et al.* 2023). There are also limited molecular markers related to plant height available for molecular-assisted breeding.

Our study used proteomic methods to obtain numerous regulatory proteins in different tissues at the jointing stage (Table 1). In total, 7,252, 7,183, and 4,637 proteins were identified in the nodes, leaves, and internodes, respectively (Fig. 2). We also uncovered 18,441, 8,152, 35,046, 38,373, 11,009, and 25,119 *de novo*-sequenced peptides in these three tissues of Ci846 and Yugu 18, respectively, suggesting their presence in foxtail millet but their absence in current transcriptome databases. Therefore, we performed a multi-round search using the monocotyledonous plant proteins database and found 1,005, 2,127, 948, 305, 2,337, and 1,595 peptides in addition to 629, 1,062, 565, 227, 1,210, and 839 protein groups. This finding indicates that *de novo* sequencing greatly increases the number of proteins obtained by shotgun identification and further improves transcriptomic data.

4.2. Analysis of the PPI networks and regulation of protein modification, including phosphorylation, ubiquitination or neddylation, in the context of plant height determination

Through the analysis of PPI networks, we discovered that SiRUB1s (known as NEDD8) are abundant in Yugu 18 and potentially interact with CUL1, CUL2, and CUL3A (Appendix P-c and d). Given that CUL1 is a component of SCF ubiquitin ligase complexes involved in the auxin response (Yu *et al.* 2015), this suggests that SiRUB1s might regulate plant height by interacting with CUL1 and modulating auxin levels or signaling pathways. Our analysis also revealed the enrichment of SiPP2C in the nodes of Ci846 (Appendix S-d), a member of the protein phosphorylation family known for its negative regulation of ABA signaling pathways (Brookbank *et al.* 2021). Notably, SiPP2C appears to interact with BIN2, BIL1, ASK11, ASK12, ASK31, ASK41, and ASK42 (Appendix S-e), which are homologous genes that negatively modulate the BR signaling pathway (Yan *et al.* 2009). Since BIN2 is known to regulate plant height in wheat (Dong *et al.* 2023), it is intriguing to speculate whether SiPP2C could interact with and dephosphorylate BIN2, thus inhibiting its activity and activating BR signaling to regulate plant height. Furthermore, the role of SiPP2C in the crosstalk between the ABA and BR signaling pathways remains to be elucidated and merits further investigation.

Phosphorylation, ubiquitination, and neddylation participate in various cellular processes, including health and diseases, drug responses, and plant growth and development (Li and Liu 2021; Pellegrino *et al.* 2022). ZmTE1 is a key regulator of plant height that can regulate the orderly formation of internode meristems and rapid cell elongation. Protein kinase ZmWEE1 and phosphatase ZmPP2Ac-2 balance the activity of ZmTE1 through its phosphorylation (Wang *et al.* 2022). These reports indicate that protein modifications play an important role in plant height regulation, but the related mechanism needs further study. Our study found that ubiquitination or neddylation was enriched in Yugu 18 (Appendix P-a), and the neddylation-related proteins SiRUB1s were also enriched in Yugu 18 (Appendix P-c). In addition, phosphorylation and dephosphorylation were

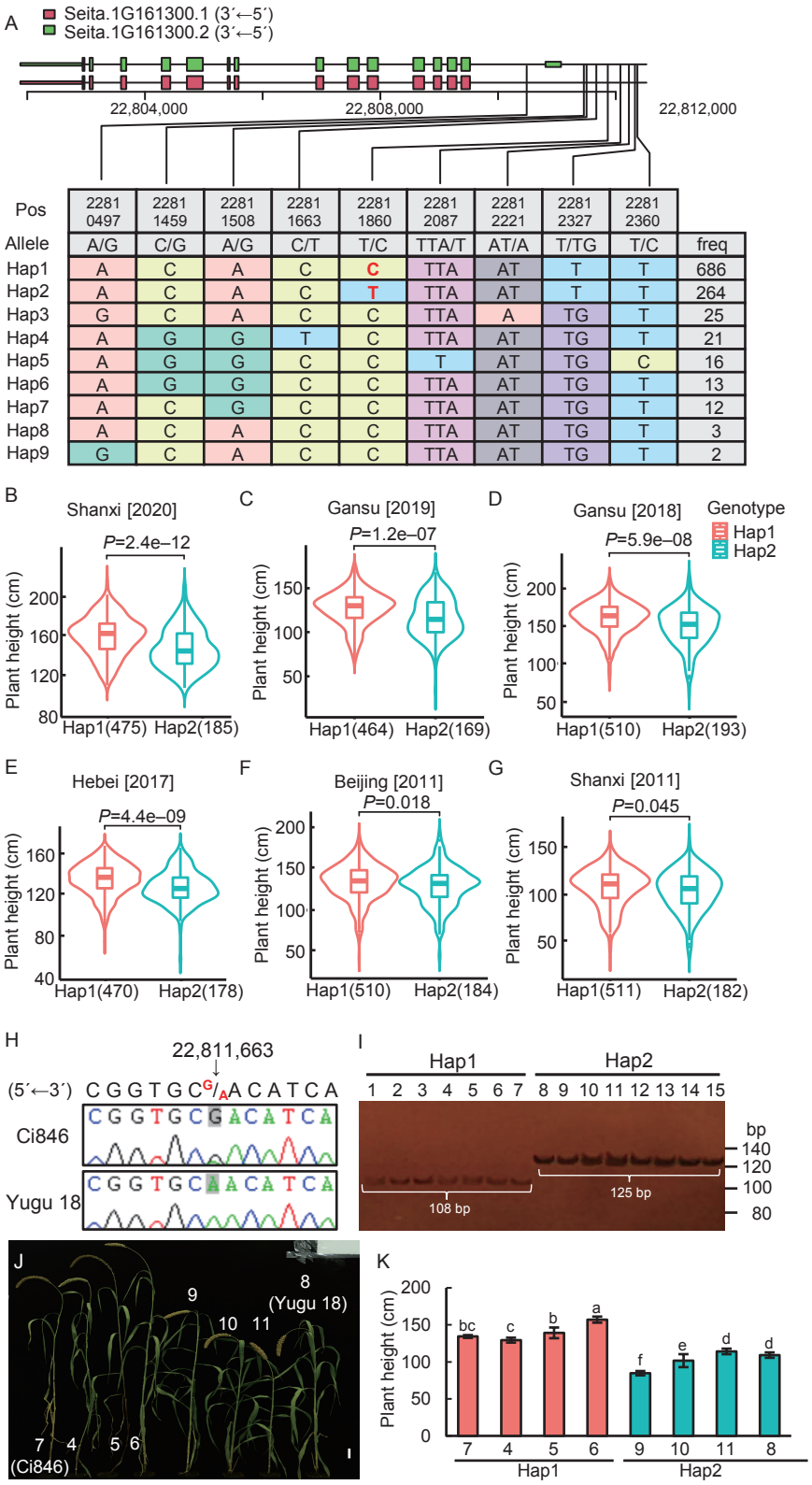


Fig. 5 Haplotype analysis and functional marker development of *SiSAUR-like*. A, gene structure and SNP polymorphism of the promoter (3′←5′) of *SiSAUR-like* (*Seita.1G161300*). The red bases represent key SNP variants, freq represents the number of millet varieties occupied by haplotype. B–G, correlation analysis of *SiSAUR-like* haplotypes with plant height in multiple locations and multi-year fractions in Shanxi, Gansu, Beijing, and Hebei, China. The numbers represent the number of millet varieties in Hap1, and Hap2. H, sanger sequencing of the promoter (5′←3′) of *SiSAUR-like* in Ci846 and Yugu 18. I, the Hpy99I digested PCR fragment patterns of different materials from different haplotypes. Polymorphic PCR bands were observed using the *Hpy*99I restriction endonucleases, Hap1 (1–7) were 108 and 17 bp, and Hap2 (8–15) were 125 bp. 1, Paoziyanguzi 1; 2, Maotigu; 3, Longzhuanian; 4, Qingruangu; 5, Xiaohonggu; 6, Chigu 7; 7, Ci846; 8, Yugu 18; 9, Ai88; 10, Mengfenggu 11; 11, Huangtoubang; 12, Jigu 19; 13, Gongai 2; 14, Dazaopi; 15, Longgu 31. J, phenotypes of Hap1 (4–7) and Hap2 (8–11). Bar=6.5 cm. K, the plant height of J. Error bars indicate ±SD of n=7. Statistically significant differences are indicated by different lowercase letters (P<0.05, one-way ANOVA with Tukey's significant difference test).

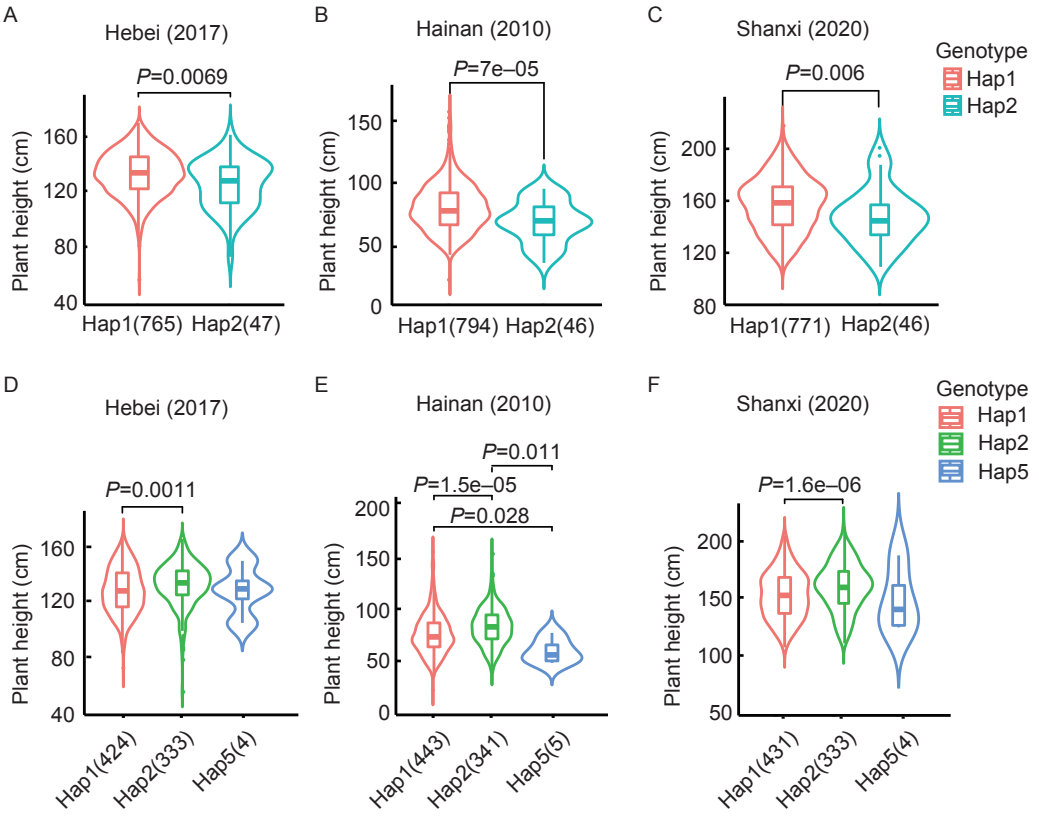


Fig. 6 Correlation analysis and geographical distribution of *SiTCH4* and *SiGH3* haplotypes with plant height. A–C, correlation analysis of *SiTCH4* (*Seita.4G246400*) haplotypes with plant height among Hebei, Hainan, and Shanxi, China. D–F, correlation analysis of *SiGH3* (*Seita.5G342900*) haplotypes with plant height among Hebei, Hainan, and Shanxi, China.

enriched in nodes, and in 1,464 proteins of Ci846 (Appendices P-b and S-b). The phosphatases enriched in Ci846 were SiPP2C, SiPEN2, and SiPP2A (Appendices P-b, -d and S-d), which may play protein-modifying roles in the auxin, ABA, BR and other plant hormone signaling pathways to affect plant height. These findings may also have implications for the balance of plant height and agronomic traits. Some reports found that neddylation of PTEN regulates its nuclear import and promotes tumor development (Xie *et al.* 2021). This discovery introduces a fresh perspective for enhancing our understanding of plant height regulation, although it remains unknown whether SiRUB1s interact with SiPEN2 or whether they play a role in the plant height regulatory mechanism.

4.3. Plant hormone signaling, carbon metabolism and biosynthesis of amino acids pathways play essential roles at the jointing stage of foxtail millet

Plant hormones play essential roles in plant growth and development by regulating diverse processes such as cell elongation and division, cell senescence, photomorphogenesis, seed germination, and abiotic and biotic stress responses, especially in plant height regulation (Nolan *et al.* 2019). However, most previous research has focused on the overall height of plants after maturity, and there is a lack of in-depth exploration of the regulatory mechanisms during early development. Moreover, plant height is determined by the number and length of internodes. Hence, our study focused on analyzing internodes, nodes, and leaves at the jointing stage to investigate the mechanism of plant height regulation in foxtail millet. Specifically, we determined the key genes at the jointing stage. Our findings offer valuable insights for understanding the molecular mechanisms governing plant height in foxtail millet, with potential applications in other crops.

Our research revealed that the number of proteins in nodes at the jointing stage was basically the same as that in leaves but much larger than that in internodes (Fig. 2; Appendix V). This may be due to the uniformity of cells in the internode tissue. The KEGG pathway analysis showed that the proteins identified in internodes, nodes, and leaves were enriched to different degrees in the same processes, such as the MAPK signaling pathway, plant hormone signal transduction, fatty acid metabolism and degradation, and others (Fig. 2-D and E). Among them, plant hormone signal transduction and fatty acid metabolism are known to be involved in the regulation of plant height (Liu *et al.* 2018). Moreover, there were more hormone-related proteins in nodes and leaves than in internodes, suggesting a stronger role for hormones in node and leaf development during the jointing stage (Appendix V). Specifically, the GA synthetic genes and signaling pathway have been reported to regulate plant height. We found that proteins related to the GA signaling pathway in foxtail millet were concentrated in nodes and leaves but not in internodes at the jointing stage (Appendices R and V). This indicates that the GA signaling pathway functions mainly in the nodes

and leaves, instead of the internodes, during the jointing stage of foxtail millet, highlighting the functional differences among different tissues.

In addition, more genes related to the ethylene signaling pathway were identified in Ci846, in either nodes or internodes (Appendices R and U). A 1-aminocyclopropane-1-carboxylic acid synthase (ACC) gene (*ACS*) is involved in ethylene biosynthesis. Overexpression of *ACS* results in dwarfing phenotypes in tobacco and lemon with increased ethylene release and reduced gibberellin content. The ACS-ERF3 complex is involved in the regulation of plant height by regulating the expression levels of *CiGA20ox1* and *CiGA20ox2* in citrus (Chu *et al.* 2023). A lower ethylene content in sugarcane resulted in greater plant height, the expression of growth-promoting genes, higher photosynthetic rates, and increased antioxidant compounds (Neris *et al.* 2022). In wheat overexpressing *TaERF8-2*, a new member of the ERF family, plant height decreased significantly, heading date advanced, and 1,000-grain weight increased (Zhang *et al.* 2020). In conclusion, ethylene plays an important role in regulating plant height in various species. Therefore, ethylene may also have a potential effect on controlling plant height in foxtail millet.

Carbon metabolism is the most important basic metabolic pathway in plants, providing the necessary carbon skeleton and energy for amino acid, protein and nucleic acid synthesis in nitrogen metabolism. Interestingly, we found that the carbon metabolism and biosynthesis of amino acids pathways had the most differences between Yugu 18 and Ci846 (Fig. 2-D and E). Following a careful analysis, we found six proteins (Seita.1G315800, Seita.2G137100, Seita.5G314300, Seita.6G159300, Seita.6G162900, and Seita.9G064200) enriched in the carbon metabolism pathway of Yugu 18, and two proteins (Seita.1G315800 and Seita.3G375200) enriched in the biosynthesis of amino acids pathway of Yugu 18; but 51 proteins enriched in the carbon metabolism pathway of Ci846, and 47 proteins enriched in the biosynthesis of amino acids pathway of Ci846. However, considering that the number of proteins enriched in Yugu 18 (336) is less than Ci846 (1,987), the numbers of carbon metabolism and amino acid biosynthesis pathway enriched proteins in Ci846 represented 2.6% (51 out of 1,987) and 2.4% (46 out of 1,987), which were significantly higher than those in Yugu 18 (1.8% (6 out of 336) and 0.6% (2 out of 336)). This suggests the significant enrichment of carbon metabolism and amino acid biosynthetic pathways in the internodes of Ci846. Specifically, all these enriched proteins were found to be enzymes that play important roles in carbon and amino acid synthesis and metabolism. This implies that the greater plant height of Ci846 may be due to an increase in the number of enzymes involved in carbon metabolic processes and the variety of enzymes related to amino acid synthesis in the internodes, which accelerates nitrogen utilization as well as amino acid requirements for the processes of growth and development. In summary, our study initially found that the increases in various enzymes in the carbon metabolism and biosynthesis of amino acids pathways may have a determining effect on plant height, but the specific mechanism of action of these enzymes needs to be investigated further in the future.

4.4. Auxin and BR signaling pathways are important regulators of plant height at the jointing stage

The genetic resources of foxtail millet can be divided into spring-sowing ecotypes and summer-sowing ecotypes according to their geographical distribution and sowing time. The existing evidence shows that the average heading time of spring-sowing foxtail millet is obviously earlier than that of summer-sowing ecotypes. However, studies on the plant height differences between these two kinds of foxtail millet have not been reported (Jia *et al.* 2013). We found that the plant height measurements of the spring-sowing genotype Ci846 were significantly greater than those of the summer-sowing cultivar Yugu 18 at the jointing stage, including the number of internodes, the length of internodes and the length of young leaves (Fig. 1). Notably, internode length is primarily determined by the elongation of intercalary cells. Our research revealed a total of 47 and 23 identified proteins enriched in the BR and auxin pathways, respectively, both of which play a pivotal role in regulating cell elongation (Appendix V).

ARFs play crucial roles in the auxin-mediated response, and 24 SiARF genes have been identified in foxtail millet (Chen *et al.* 2021). Our proteomic data identified 14 SiARF homologous genes, which were enriched not only in the nodes and leaves but also in the internodes; in addition, almost all of them were in the internodes of Ci846 (Fig. 3-A; Appendix V). These genes are highly expressed in the stem (Chen *et al.* 2021), and activity-elevated ARFs regulate the expression of auxin-related response genes such as *SAUR* and *GH3* (Tiwari *et al.* 2003). Consistent with this, in contrast to Ci846, the genes downregulated in Yugu 18 were also enriched in the response to auxin and auxin-activated signaling pathways (Fig. 3-C and D). qRT-PCR also verified that the *SiSAURs* were indeed down-regulated in Yugu 18 (Fig. 4). While the IAA content in Yugu 18 was significantly higher than that in Ci846 (Fig. 3-B), these findings indicated that the high content of auxin in Yugu 18 inhibited the auxin signaling pathway thereby suppressing the expression of downstream-regulated genes. In conclusion, the proper auxin content is essential for activating downstream gene expression and thus regulating plant height.

The haplotype analysis of *SiSAUR-like* showed that only two important haplotypes were associated with plant height (Fig. 5-B–G). The functional dCAPS marker *SiSAUR-like* (*SiSAUR-like*-FCM1-2) can be used to efficiently distinguish accessions with Hap1 and Hap2 in Ci846, Yugu 18, and natural populations, indicating that *SiSAUR-like*-FCM1-2 will greatly aid in the breeding of foxtail millet (Fig. 5-H and I). Besides identifying SiSAUR-like as a pivotal gene in plant height regulation, our research highlighted the significant roles of SiGH3 and SiTCH4 in the auxin and BR signaling pathways, respectively (Fig. 6-A–F; Appendix V). Notably, SiTCH4 and SiGH3 were specifically identified in the internodes of Ci846 (Appendix V), indicating that SiTCH4 and SiGH3 are indeed key genes in plant height regulation. In summary, the downstream regulatory factors SiSAURs, SiGH3, and SiTCH4 play a dual role in plant height regulation by influencing both transcription and, notably, protein-level internode cell elongation. These findings hold great significance for future breeding efforts.

4.5. Integration of the plant hormone signaling pathway by key genes that regulate plant height

Plant height regulation involves the elaborate interplay of various plant hormones. For instance, the Aux/IAA family gene *OsIAA1* assumes a significant role in mediating crosstalk between the auxin and BR signaling pathways (Song *et al.* 2009). In addition, the ABA-induced gene *OsREM4.1* interacts with OsSERK1 to facilitate the integration of ABA and BR signaling (Gui *et al.* 2016). The ETH-response AP2/ERF factor OsEATB restricts internode elongation by suppressing the GA biosynthetic gene (Qi *et al.* 2011). Moreover, the ABA-responsive element binding factor OsABF1 recruits PRC2-mediated H3K27me3 deposition on the SD1 promoter to maintain GA homeostasis (Tang *et al.* 2021).

Despite the significant role attributed to GA as a primary hormone associated with plant height, our data reveals an intriguing trend. The numbers of enriched proteins and DEGs in the auxin pathway were significantly higher than those observed in the GA pathway (Appendix BB). This suggests that the primary hormones regulating plant height vary depending on the stage and tissue being considered. Notably, within the auxin pathway, proteomic enrichment proteins are primarily clustered around transcription factors, particularly ARFs. On the other hand, the DEGs identified through RNAseq are concentrated in *AUX/IAA*, *GH3*, and *SAUR*, which are downstream targets of ARFs (Appendix BB). These observations align closely with the mechanism of plant height regulation *via* SiARFs-SiSAURs that we described previously.

Furthermore, BR regulates leaf drooping and induces the expression of the cell elongation-associated target gene SAUR (Zhao *et al.* 2020; Chai *et al.* 2022). Whether this is related to BR negative feedback regulation is unknown. Therefore, further investigation is needed to determine whether SiSAURs are co-regulated by both auxin and BR in the process of plant height control. Furthermore, SiPP2C plays an important regulatory role in the ABA and BR hormone signaling pathways (Appendix S), as well as ubiquitination. The protein-level regulation of these key components in the auxin and BR signaling pathways responsible for plant height remains uncertain. The regulation of these proteins at the level of protein modification requires further study.

Reduced plant height can increase lodging resistance and consequently improve yield potential and stability. However, when plants become over-dwarf, the yield is negatively affected, so achieving a balance between plant height and various agronomic traits is the key to future breeding success. The original findings of our study and the new *SiSAUR-like* marker will facilitate the study and characterization of plant height and contribute to the development of new cereal varieties with ideal plant heights through target based editing and marker-assisted selection.

5. Conclusion

Plant height is a fundamental agronomic trait, and achieving an optimal plant height is crucial for maximizing crop yield. This study provides a high-quality shotgun proteomics analysis of the node, internode and leaf in foxtail millet, and proteins related to plant hormones, especially auxin signaling, were significantly enriched in the jointing stage. Furthermore, through transcriptomics, auxin concentration analysis and qRT-PCR, we discovered that auxin may regulate the expression level of *SiSAUR-like* through SiARFs, further controlling the elongation of the internodes in Ci846. Finally, by haplotype and phenotypic association analyses, we found that the genotypic variations of *SiSAUR-like* determine plant height at the jointing stage.

Acknowledgements

This work was supported by the grants from the National Natural Science Foundation of China (32241042), the Science Research Project of Hebei Education Department, China (BJ2021029), the Natural Science Foundation for Excellent Youth Scholars of Hebei Province, China (C2021205011), and the Graduate innovation Funding Project of Hebei Normal University, China (XCXZZSS202337). We thank American Journal Experts (www.aje.com) for their linguistic assistance during the preparation of this manuscript.

Declaration of competing interest

The authors declare that they have no conflict of interest.

Declaration of generative AI and AI-assisted technologies in the writing process

The authors declare that they did not use AI in the preparation and writing of this manuscript.

Appendices associated with this paper are available at https://doi.org/10.1016/j.jia.2024.06.014

References

Ashikari M, Sakakibara H, Lin S, Yamamoto T, Takashi T, Nishimura A, Angeles E R, Qian Q, Kitano H, Matsuoka M. 2005. Cytokinin oxidase regulates rice grain production. *Science*, **309**, 741–745.

Best N B, Hartwig T, Budka J, Fujioka S, Johal G, Schulz B, Dilkes B P. 2016. *nana plant2* encodes a maize ortholog of the *Arabidopsis* brassinosteroid biosynthesis gene *DWARF1*, identifying developmental interactions between brassinosteroids and gibberellins. *Plant Physiology*, **171**, 2633–2647.

Bostick M, Lochhead S R, Honda A, Palmer S, Callis J. 2004. Related to ubiquitin 1 and 2 are redundant and essential and regulate vegetative growth, auxin signaling, and ethylene production in *Arabidopsis*. *The Plant Cell*, **16**, 2418–2432.

Brookbank B P, Patel J, Gazzarrini S, Nambara E. 2021. Role of basal ABA in plant growth and development. *Genes* (Basel), **12**, 1936.

Chai G, Qi G, Wang D, Zhuang Y, Xu H, Bai Z, Bai MY, Hu R, Wang Z Y, Zhou G, Kong Y. 2022. The CCCH zinc finger protein C3H15 negatively regulates cell elongation by inhibiting brassinosteroid signaling. *Plant Physiology*, **189**, 285–300.

Chen Y, Liu B, Zhao Y, Yu W, Si W. 2021. Whole-genome duplication and purifying selection contributes to the functional redundancy of auxin response factor (ARF) genes in foxtail millet (*Setaria italica* L.). *International Journal of Genomics*, **2021**, 2590665.

Christians M J, Rottier A, Wiersma C. 2018. Light regulates the RUBylation levels of individual cullin proteins in *Arabidopsis thaliana*. *Plant Molecular Biology Reporter*, **36**, 123–134.

Chu J, Fang S, Xin P, Guo Z, Chen Y. 2017. Quantitative analysis of plant hormones based on LC-MS/MS. In: Li J, Li C, Smith S M, eds., *Hormone Metabolism and Signaling in Plants*. Elsevier, London. pp. 471–537.

Chu L, Yan Z, Sheng X, Liu H, Wang Q, Zeng R, Hu C, Zhang J. 2023.

Citrus ACC synthase CiACS4 regulates plant height by inhibiting gibberellin biosynthesis. *Plant Physiology*, **192**, 1947–1968.
Diao X, Jia G. 2017. Foxtail millet breeding in China. In: Doust A, Diao X, eds., *Genetics and Genomics of Setaria*. Springer, Cham. pp. 93–113.
Diao X, Schnable J, Bennetzen L J, Li J. 2014. Initiation of Setaria as a model plant. *Frontiers of Agricultural Science and Engineering*, **1**, 16–20.
Dong H, Li D, Yang R, Zhang L, Zhang Y, Liu X, Kong X, Sun J. 2023. GSK3 phosphorylates and regulates the green revolution protein Rht-B1b to reduce plant height in wheat. *The Plant Cell*, **35**, 1970–1983.
Enchev R I, Schulman B A, Peter M. 2015. Protein neddylation: Beyond cullin–RING ligases. *Nature Reviews Molecular Cell Biology*, **16**, 30–44.
Fan X, Tang S, Zhi H, He M, Ma W, Jia Y, Zhao B, Jia G, Diao X. 2017. Identification and fine mapping of SiDWARF3(D3), a pleiotropic locus controlling environment-independent dwarfism in foxtail millet. *Crop Science*, **57**, 2431–2442.
Ford B A, Foo E, Sharwood R, Karafiatova M, Vrana J, MacMillan C, Nichols D S, Steuernagel B, Uauy C, Dolezel J, Chandler P M, Spielmeyer W. 2018. *Rht18* Semidwarfism in wheat is due to increased *GA 2-oxidaseA9* expression and reduced GA content. *Plant Physiology*, **177**, 168–180.
Gui J, Zheng S, Liu C, Shen J, Li J, Li L. 2016. OsREM4.1 interacts with OsSERK1 to coordinate the interlinking between abscisic acid and brassinosteroid signaling in rice. *Developmental Cell*, **38**, 201–213.
Guo F, Huang Y, Qi P, Lian G, Hu X, Han N, Wang J, Zhu M, Qian Q, Bian H. 2021. Functional analysis of auxin receptor OsTIR1/OsAFB family members in rice grain yield, tillering, plant height, root system, germination, and auxinic herbicide resistance. *New Phytologist*, **229**, 2676–2692.
Guo G, Li N. 2011. Relative and accurate measurement of protein abundance using ^{15}N stable isotope labeling in *Arabidopsis* (SILIA). *Phytochemistry*, **72**, 1028–1039.
Gupta R, Ting J T, Sokolov L N, Johnson S A, Luan S. 2002. A tumor suppressor homolog, AtPTEN1, is essential for pollen development in *Arabidopsis*. *The Plant Cell*, **14**, 2495–2507.
Hartwig T, Chuck G S, Fujioka S, Klempien A, Weizbauer R, Potluri D P, Choe S, Johal G S, Schulz B. 2011. Brassinosteroid control of sex determination in maize. *Proceedings of the National Academy of Sciences of the United States of America*, **108**, 19814–19819.
He Q, Tang S, Zhi H, Chen J, Zhang J, Liang H, Alam O, Li H, Zhang H, Xing L, Li X, Zhang W, Wang H, Shi J, Du H, Wu H, Wang L, Yang P, Xing L, Yan H, *et al.* 2023. A graph-based genome and pan-genome variation of the model plant Setaria. *Nature Genetics*, **55**, 1232–1242.
He Q, Zhi H, Tang S, Xing L, Wang S, Wang H, Zhang A, Li Y, Gao M, Zhang H, Chen G, Dai S, Li J, Yang J, Liu H, Zhang W, Jia Y, Li S, Liu J, Qiao Z, *et al.* 2021. QTL mapping for foxtail millet plant height in multi-environment using an ultra-high density bin map. *Theoretical and Applied Genetics*, **134**, 557–572.
Huo C, Zhang B, Wang H, Wang F, Liu M, Gao Y, Zhang W, Deng Z, Sun D, Tang W. 2016. Comparative study of early cold-regulated proteins by two-dimensional difference gel electrophoresis reveals a key role for Phospholipase Dα1 in mediating cold acclimation signaling pathway in rice. *Molecular & Cellular Proteomics*, **15**, 1397–1411.
Iliev E A, Xu W, Polisensky D H, Oh M H, Torisky R S, Clouse S D, Braam J. 2002. Transcriptional and posttranscriptional regulation of Arabidopsis *TCH4* expression by diverse stimuli. Roles of *cis* regions and brassinosteroids. *Plant Physiology*, **130**, 770–783.
Jia G, Huang X, Zhi H, Zhao Y, Zhao Q, Li W, Chai Y, Yang L, Liu K, Lu H, Zhu C, Lu Y, Zhou C, Fan D, Weng Q, Guo Y, Huang T, Zhang L, Lu T, Feng Q, *et al.* 2013. A haplotype map of genomic variations and genome-wide association studies of agronomic traits in foxtail millet (*Setaria italica*). *Nature Genetics*, **45**, 957–961.
Kir G, Ye H, Nelissen H, Neelakandan A K, Kusnandar A S, Luo A, Inzé D, Sylvester A W, Yin Y, Becraft P W. 2015. RNA interference knockdown of BRASSINOSTEROID INSENSITIVE1 in maize reveals novel functions for brassinosteroid signaling in controlling plant architecture. *Plant Physiology*, **169**, 826–839.
Lata C, Gupta S, Prasad M. 2013. Foxtail millet: A model crop for genetic and genomic studies in bioenergy grasses. *Critical Reviews in Biotechnology*, **33**, 328–343.
Li H, Wang L, Liu M, Dong Z, Li Q, Fei S, Xiang H, Liu B, Jin W. 2020. Maize plant architecture is regulated by the ethylene biosynthetic gene *ZmACS7*. *Plant Physiology*, **183**, 1184–1199.
Miao L, Wang X, Yu C, Ye C, Yan Y, Wang H. 2024. What factors control plant height? *Journal of Integrative Agriculture*, **23**, 1803–1824.
Li P, Liu J. 2021. Protein phosphorylation in plant cell signaling. *Methods in Molecular Biology*, **2358**, 45–71.
Li Z, Zhang X, Zhao Y, Li Y, Zhang G, Peng Z, Zhang J. 2018. Enhancing auxin accumulation in maize root tips improves root growth and dwarfs plant height. *Plant Biotechnology Journal*, **16**, 86–99.
Liang H, He Q, Zhang H, Zhi H, Tang S, Wang H, Meng Q, Jia G, Chang J, Diao X. 2023. Identification and haplotype analysis of SiCHLI: A gene for yellow-green seedling as morphological marker to accelerate foxtail millet (*Setaria italica*) hybrid breeding. *Theoretical and Applied Genetics*, **136**, 24.
Liu F, Wang P, Zhang X, Li X, Yan X, Fu D, Wu G. 2018. The genetic and molecular basis of crop height based on a rice model. *Planta*, **247**, 1–26.
Liu X, Tang S, Jia G, Schnable J C, Su H, Tang C, Zhi H, Diao X. 2016. The C-terminal motif of SiAGO1b is required for the regulation of growth, development and stress responses in foxtail millet (*Setaria italica* (L.) P. Beauv). *Journal of Experimental Botany*, **67**, 3237–3249.
Liu Y H, Sun T, Li Y Y, Huang J Q, Wang X J, Bai H M, Hu J Y, Zhang Z F, Wang S, Zhang D M, Li X X, Wang Z H, Zheng H K, Lin G F. 2025. Proteomic analysis revealed the function of PoElp3 in development, pathogenicity, and autophagy through the tRNA-mediated translation efficiency in the rice blast fungus. *Journal of Integrative Agriculture*, **24**, 1515–1528.
Mergner J, Kuster B, Schwechheimer C. 2017. DENEDDYLASE1 protein counters automodification of neddylating enzymes to maintain NEDD8 protein homeostasis in *Arabidopsis*. *Journal of Biological Chemistry*, **292**, 3854–3865.
Neris D, Mattiello L, Zuñiga G, Purgatto E, Menossi M. 2022. Reduction of ethylene biosynthesis in sugarcane induces growth and investment in the non-enzymatic antioxidant apparatus. *Plant Cell Reports*, **41**, 979–993.
Nibau C, Tao L, Levasseur K, Wu H M, Cheung A Y. 2013. The *Arabidopsis* small GTPase AtRAC7/ROP9 is a modulator of auxin and abscisic acid signalling. *Journal of Experimental Botany*, **64**, 3425–3437.
Nolan T M, Vukašinović N, Liu D, Russinova E, Yin Y. 2019. Brassinosteroids: Multi-dimensional regulators of plant growth, development, and stress responses. *The Plant Cell*, **32**, 295–318.
Pan J, Li Z, Wang Q, Garrell A K, Liu M, Guan Y, Zhou W, Liu W. 2018. Comparative proteomic investigation of drought responses in foxtail millet. *BMC Plant Biology*, **18**, 315.
Pan J, Li Z, Wang Q, Guan Y, Li X, Huangfu Y, Meng F, Li J, Dai S, Liu W. 2021. Phosphoproteomic profiling reveals early salt-responsive mechanisms in two foxtail millet cultivars. *Frontiers in Plant Science*, **12**, 712257.
Panchal A, Singh R K, Prasad M. 2023. Recent advancements and future perspectives of foxtail millet genomics. *Plant Growth Regulation*, **99**, 11–23.
Pellegrino N E, Guven A, Gray K, Shah P, Kasture G, Nastke M D, Thakurta A, Gesta S, Vishnudas V K, Narain N R, Kiebish M A. 2022. The next frontier: Translational development of Ubiquitination, SUMOylation, and NEDDylation in cancer. *International Journal of Molecular Sciences*, **23**, 3480.
Peng J, Richards D E, Hartley N M, Murphy G P, Devos K M, Flintham J E, Beales J, Fish L J, Worland A J, Pelica F, Sudhakar D, Christou P, Snape J W, Gale M D, Harberd N P. 1999. 'Green revolution' genes encode mutant gibberellin response modulators. *Nature*, **400**, 256–261.
Pribat A, Sormani R, Rousseau-Gueutin M, Julkowska M M, Testerink C, Joubès J, Castroviejo M, Laguerre M, Meyer C, Germain V, Rothan C. 2012. A novel class of PTEN protein in *Arabidopsis* displays unusual phosphoinositide phosphatase activity and efficiently binds phosphatidic acid. *Biochemical Journal*, **441**, 161–171.
Qi W, Sun F, Wang Q, Chen M, Huang Y, Feng YQ, Luo X, Yang J. 2011. Rice ethylene-response AP2/ERF factor *OsEATB* restricts internode elongation by down-regulating a gibberellin biosynthetic gene. *Plant Physiology*, **157**, 216–228.

Sasaki A, Ashikari M, Ueguchi-Tanaka M, Itoh H, Nishimura A, Swapan D, Ishiyama K, Saito T, Kobayashi M, Khush G S, Kitano H, Matsuoka M. 2002. Green revolution: A mutant gibberellin-synthesis gene in rice. *Nature*, **416**, 701–702.

Sasaki A, Itoh H, Gomi K, Ueguchi-Tanaka M, Ishiyama K, Kobayashi M, Jeong D H, An G, Kitano H, Ashikari M, Matsuoka M. 2003. Accumulation of phosphorylated repressor for gibberellin signaling in an F-box mutant. *Science*, **299**, 1896–1898.

Schwechheimer C. 2018. NEDD8-its role in the regulation of Cullin-RING ligases. *Current Opinion in Plant Biology*, **45**, 112–119.

Shi F, Wang M, An Y. 2020. Overexpression of a B-type cytokinin response regulator (OsORR2) reduces plant height in rice. *Plant Signaling & Behavior*, **15**, 1780405.

Song Y, You J, Xiong L. 2009. Characterization of OsIAA1 gene, a member of rice Aux/IAA family involved in auxin and brassinosteroid hormone responses and plant morphogenesis. *Plant Molecular Biology*, **70**, 297–309.

Spielmeyer W, Ellis M H, Chandler P M. 2002. Semidwarf (sd-1), "green revolution" rice, contains a defective gibberellin 20-oxidase gene. *Proceedings of the National Academy of Sciences of the United States of America*, **99**, 9043–9048.

Tanabe S, Ashikari M, Fujioka S, Takatsuto S, Yoshida S, Yano M, Yoshimura A, Kitano H, Matsuoka M, Fujisawa Y, Kato H, Iwasaki Y. 2005. A novel cytochrome P450 is implicated in brassinosteroid biosynthesis via the characterization of a rice dwarf mutant, *dwarf11*, with reduced seed length. *The Plant Cell*, **17**, 776–790.

Tang L, Xu H, Wang Y, Wang H, Li Z, Liu X, Shu Y, Li G, Liu W, Ying J, Tong X, Yao J, Xiao W, Tang S, Ni S, Zhang J. 2021. OsABF1 represses gibberellin biosynthesis to regulate plant height and seed germination in rice (*Oryza sativa* L.). *International Journal of Molecular Sciences*, **22**, 12220.

Teng F, Zhai L, Liu R, Bai W, Wang L, Huo D, Tao Y, Zheng Y, Zhang Z. 2013. ZmGA3ox2, a candidate gene for a major QTL, *qPH3.1*, for plant height in maize. *The Plant Journal*, **73**, 405–416.

Tian P, Liu J, Yan B, Zhou C, Wang H, Shen R. 2023. BRASSINOSTEROID–SIGNALING KINASE1–1, a positive regulator of brassinosteroid signalling, modulates plant architecture and grain size in rice. *Journal of Experimental Botany*, **74**, 283–295.

Tian X, Xia X, Xu D, Liu Y, Xie L, Hassan M A, Song J, Li F, Wang D, Zhang Y, Hao Y, Li G, Chu C, He Z, Cao S. 2022. *Rht24b*, an ancient variation of *TaGA2ox-A9*, reduces plant height without yield penalty in wheat. *New Phytologist*, **233**, 738–750.

Tiwari S B, Hagen G, Guilfoyle T. 2003. The roles of auxin response factor domains in auxin-responsive transcription. *The Plant Cell*, **15**, 533–543.

Van De Velde K, Thomas S G, Heyse F, Kaspar R, Van Der Straeten D, Rohde A. 2021. N-terminal truncated RHT-1 proteins generated by translational reinitiation cause semi-dwarfing of wheat Green Revolution alleles. *Molecular Plant*, **14**, 679–687.

Voorend W, Nelissen H, Vanholme R, De Vliegher A, Van Breusegem F, Boerjan W, Roldán-Ruiz I, Muylle H, Inzé D. 2016. Overexpression of *GA20-OXIDASE1* impacts plant height, biomass allocation and saccharification efficiency in maize. *Plant Biotechnology Journal*, **14**, 997–1007.

Wang B, Chu J, Yu T, Xu Q, Sun X, Yuan J, Xiong G, Wang G, Wang Y, Li J. 2015. Tryptophan-independent auxin biosynthesis contributes to early embryogenesis in *Arabidopsis*. *Proceedings of the National Academy of Sciences of the United States of America*, **112**, 4821–4826.

Wang F, Yu Z, Zhang M, Wang M, Lu X, Liu X, Li Y, Zhang X, Tan BC, Li C, Ding Z. 2022. ZmTE1 promotes plant height by regulating intercalary meristem formation and internode cell elongation in maize. *Plant Biotechnology Journal*, **20**, 526–537.

Winkler R G, Helentjaris T. 1995. The maize *Dwarf3* gene encodes a cytochrome P450-mediated early step in gibberellin biosynthesis. *The Plant Cell*, **7**, 1307–1317.

Wu J, Kong X, Wan J, Liu X, Zhang X, Guo X, Zhou R, Zhao G, Jing R, Fu X, Jia J. 2011. Dominant and pleiotropic effects of a GAI gene in wheat results from a lack of interaction between DELLA and GID1. *Plant Physiology*, **157**, 2120–2130.

Würschum T, Langer S M, Longin C F H, Tucker M R, Leiser W L. 2017. A modern Green Revolution gene for reduced height in wheat. *The Plant Journal*, **92**, 892–903.

Xie P, Peng Z, Chen Y, Li H, Du M, Tan Y, Zhang X, Lu Z, Cui CP, Liu C H, He F, Zhang L. 2021. Neddylation of PTEN regulates its nuclear import and promotes tumor development. *Cell Research*, **31**, 291–311.

Xue C, Zhi H, Fang X, Liu X, Tang S, Chai Y, Zhao B, Jia G, Diao X. 2016. Characterization and fine mapping of *SiDWARF2* (*D2*) in foxtail millet. *Crop Science*, **56**, 95.

Yan Z, Zhao J, Peng P, Chihara R K, Li J. 2009. BIN2 functions redundantly with other *Arabidopsis* GSK3-like kinases to regulate brassinosteroid signaling. *Plant Physiology*, **150**, 710–721.

Yang D, Yao J, Mei C, Tong X, Zeng L, Li Q, Xiao L, Sun T, Li J, Deng X, Lee CM, Thomashow M F, Yang Y, He Z, He S. 2012. Plant hormone jasmonate prioritizes defense over growth by interfering with gibberellin signaling cascade. *Proceedings of the National Academy of Sciences of the United States of America*, **109**, E1192–E1200.

Yang Z, Zhang H, Li X, Shen H, Gao J, Hou S, Zhang B, Mayes S, Bennett M, Ma J, Wu C, Sui Y, Han Y, Wang X. 2020. A mini foxtail millet with an *Arabidopsis*-like life cycle as a C_4 model system. *Nature Plants*, **6**, 1167–1178.

Yu H, Zhang Y, Moss B L, Bargmann B O, Wang R, Prigge M, Nemhauser J L, Estelle M. 2015. Untethering the TIR1 auxin receptor from the SCF complex increases its stability and inhibits auxin response. *Nature Plants*, **1**, 14030.

Zhang A M, Li Z H, Zhou Q R, Zhao J W, Zhao Y, Zhao M T, Ma S Y, Fan Y H, Huang Z L, Zhang W J. 2025. An integrated physiology and proteomics analysis reveals the response of wheat grain to low temperature stress during booting. *Journal of Integrative Agriculture*, **24**, 114–131.

Zhang B, Wang X, Zhao Z, Wang R, Huang X, Zhu Y, Yuan L, Wang Y, Xu X, Burlingame A L, Gao Y, Sun Y, Tang W. 2016. OsBRI1 activates BR signaling by preventing binding between the TPR and kinase domains of OsBSK3 *via* phosphorylation. *Plant Physiology*, **170**, 1149–1161.

Zhang G, Liu X, Quan Z, Cheng S, Xu X, Pan S, Xie M, Zeng P, Yue Z, Wang W, Tao Y, Bian C, Han C, Xia Q, Peng X, Cao R, Yang X, Zhan D, Hu J, Zhang Y, *et al.* 2012. Genome sequence of foxtail millet (*Setaria italica*) provides insights into grass evolution and biofuel potential. *Nature Biotechnology*, **30**, 549–554.

Zhang L, Liu P, Wu J, Qiao L, Zhao G, Jia J, Gao L, Wang J. 2020. Identification of a novel ERF gene, *TaERF8*, associated with plant height and yield in wheat. *BMC Plant Biology*, **20**, 263.

Zhang R, Jia G, Diao X. 2023. geneHapR: An R package for gene haplotypic statistics and visualization. *BMC Bioinformatics*, **24**, 199.

Zhao M, Tang S, Zhang H, He M, Liu J, Zhi H, Sui Y, Liu X, Jia G, Zhao Z, Yan J, Zhang B, Zhou Y, Chu J, Wang X, Zhao B, Tang W, Li J, Wu C, Liu X, Diao X. 2020. DROOPY LEAF1 controls leaf architecture by orchestrating early brassinosteroid signaling. *Proceedings of the National Academy of Sciences of the United States of America*, **117**, 21766–21774.

Zhao M, Zhi H, Zhang X, Jia G, Diao X. 2019. Retrotransposon-mediated DELLA transcriptional reprograming underlies semi-dominant dwarfism in foxtail millet. *The Crop Journal*, **7**, 458–468.

Zhao Z, Tang S, Li W, Yang X, Wang R, Diao X, Tang W. 2021a. Overexpression of a *BRASSINAZOLE RESISTANT 1* homolog attenuates drought tolerance by suppressing the expression of *PLETHORA-LIKE 1* in *Setaria italica*. *The Crop Journal*, **9**, 1208–1213.

Zhao Z, Tang S, Zhang Y, Yue J, Xu J, Tang W, Sun Y, Wang R, Diao X, Zhang B. 2021b. Evolutionary analysis and functional characterization of SiBRI1 as a Brassinosteroid receptor gene in foxtail millet. *BMC Plant Biology*, **21**, 291.

Zhou H, Wang X, Huo C, Wang H, An Z, Sun D, Liu J, Tang W, Zhang B. 2019. A quantitative proteomics study of early heat-regulated proteins by two-dimensional difference gel electrophoresis identified OsUBP21 as a negative regulator of heat stress responses in rice. *Proteomics*, **19**, e1900153.

Executive Editor-in-Chief Xueyong Zhang
Managing Editor Ning Wang